LOADING EFFECTS ON GAS RELATIVE PERMEABILITY OF A LOW PERMEABLE SANDSTONE

F. Agostini[1], P. Egermann[2], L. Jeannin[2], E. Portier[3], F. Skoczylas[1], Y. Wang[1]

(1) LamCube CNRS FRE 2016, and Centrale de Lille, CS20048, F-59651 Villeneuve D'Ascq Cedex, France
(2) Storengy, 12 rue Raoul Nordling - Djinn - CS 70001 92274 Bois Colombes Cedex
(3) ENGIE EPI, 1 Place Samuel de Champlain, 92930 La Défense Cedex, France

This paper was prepared for presentation at the International Symposium of the Society of Core Analysts held in Trondheim, Norway, 27-30 August 2018

ABSTRACT

This paper deals with a study of the gas relative permeability of tight sandstones under loading. Specific experiments have been designed and the experimental measurements obtained show that, not only the absolute permeability but also the gas relative permeability are sensitive to confinement and that the residual gas saturation (through permeability "jail") increases with loading. This observation consists in an additional source of complexity in the evaluation of low permeable sandstone gas reservoirs.

INTRODUCTION

Low permeable gas sandstone reservoirs, also called tight reservoirs, are generally considered as stress-sensitive reservoirs. Numerous laboratory tests under single phase flow have shown that the absolute permeability of these reservoir rocks decreases strongly with confinement. This dependence to confinement is attributed to the existence of joints and interfaces in tight rocks, which close when loading increases as pointed out by Walsh and Brace [17] and Warpinski and Teufel [20].

As two-phase flow experiments are rather time-consuming and tricky for low permeable sandstone, gas relative permeabilities are most of the time estimated without confinement variations in SCAL studies. Various measurements show that the gas relative permeability rapidly drops for a water saturation of 0.3-0.4 and becomes negligible at higher saturation [13]. A saturation region is indeed observed, where water and gas permeabilities are practically zero: this phenomenon is called "permeability jail" in the petroleum literature [3, 4, 13, 19]. However, the relative gas permeabilities may also be modified under loading evolution with the reservoir depletion. At the pore scale, some pathways allowing the flow of the gas are likely to be blocked either by the presence of water or by the closure of joints due to loading. In addition, the closure of joints may also induce a redistribution of water phase in the pore network. An understanding of the effective permeability to gas as a function of both water saturation and loading is then interesting to fully evaluate tight sand reservoirs.

In this study, specific experiments have been designed to characterize these effects for sandstone samples of a low permeable gas reservoir. The dedicated experimental set-up and protocol put in place make it possible to accurately control both the saturation of the

sample and the loading. The full measurements obtained on a series of 8 samples (from 1.5 µD down to 0.08 µD) show that both the absolute permeability and the gas relative permeabilities evolve with confinement variations. The relative gas permeabilities decrease while the residual gas saturations increase with higher loading values.

These results provide an additional complexity in the evaluation of low permeable sandstone gas reservoirs. On the one hand, the evolution of the end points of relative permeability, and mainly of the residual gas saturation, make the assessment of the recoverable volume more uncertain. On the other hand, a decrease of gas relative permeability under higher loading during depletion implies less favorable production forecasts.

The paper is organized in two main parts: The first section is dedicated to a description of the specific experimental set-ups and protocols used for tight rocks. The second part presents the experimental results related to a specific tight gas field.

EXPERIMENTAL DATA

Porosity

The total apparent volume V_{total} of a sample is measured by hydrostatic weighing. The dry mass m_{dry} is obtained by oven-drying the sample at 105ºC. Mass stabilization is assumed using a mass variation criterion, i.e. when the mass variation is less than 0.01g/week.

The bulk density ρ_{app} is then determined as the ratio of the dry mass m_{dry} and the total apparent volume:

$$\rho_{app} = \frac{m_{dry}}{V_{total}} \quad \text{(eq. 1)}$$

Water porosity of a sample is defined as follows:

$$\phi_w = \frac{m_{sat} - m_{dry}}{\rho_w V_{total}} \quad \text{(eq. 2)}$$

where m_{sat} is the water-saturated mass and ρ_w is water density. The same mass stabilization criterion is used to determine the water-saturated mass m_{sat}, the samples being fully water-saturated under vacuum at room temperature.

Sample saturation

Intermediate water saturation S_w of a sample is related to its mass m by the following equation:

$$S_w = \left(m - m_{dry}\right)/\left(m_{sat} - m_{dry}\right) \quad \text{(eq. 3)}$$

The saturation method developed by Rilem [10] for concrete samples was used to establish the initial water content. The dry sample is first water saturated until the required mass m (eq. 3) is reached. The sample is then sealed using three layers of self-adhesive aluminum and one layer of paraffin and kept in a climatic chamber at 40 ºC for

at least 14 days. The time laps allows water distribution homogenization within the sample. It has been verified that homogenization times longer than 14 days do not lead to changes in measured effective gas permeability.
The gas permeability measurement may lead to changes in the water saturation because of the production of water (due to mechanical loading and gas pressure pushing the water contained in the biggest pores). Therefore, the water saturation indicated in the following is the average saturation before and after permeability tests. It has been observed a maximum variation of 1-2% of pore space.

Gas permeability
Although the gas permeability of tight sandstone is low compared to conventional sandstone, it is nevertheless sufficiently high to be measured with quasi-stationary flow techniques [8, 15].

Gas permeability K_g is measured using a uniaxial steady state gas flow apparatus (Figure 1). The apparatus consists of a confining cell, which can reach confining pressures P_c as high as 100 MPa, together with a gas injection device. The gas used in the current study is 99%-pure Argon.

A constant injection gas pressure (P_i) is applied on one end of the sample, while the other end is at atmospheric pressure (P_0). The quasi-steady flow state method consists of measuring the average gas volume flow rate (Q_m) injected in the sample during a slight decrease (ΔP_i) of injection pressure (P_i), in a tank of known volume (V_t), connected at the entrance of the sample (see Figure 1). The mean injection gas pressure is then equal to $P_m = P_i - (\Delta P_i/2)$. Using Darcy's law, gas permeability K_g can be estimated by:

$$K_g = \frac{2.\mu.L.P_m.Q_m}{S.(P_m^2 - P_0^2)} \quad \text{(eq. 4)}$$

where μ is the dynamic viscosity of the gas, L the length of the sample and S the cross section of the sample. Steady state flow is assumed when two successive gas permeability measurements (at least 30 minutes between each one) lead to a difference smaller than 3%.

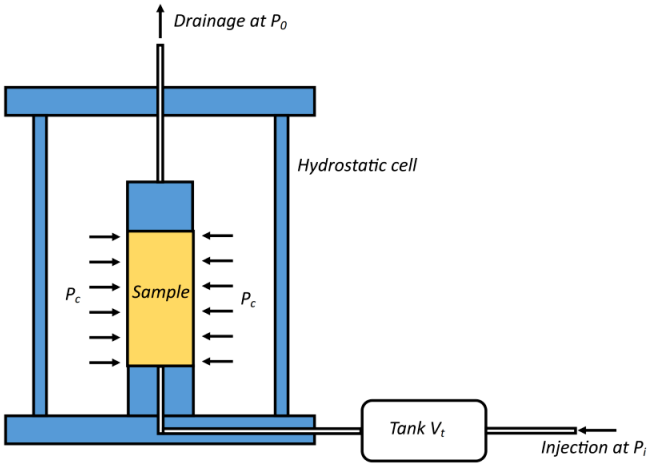

Figure 1 : Test apparatus of gas permeability

Effective permeability and relative permeability

In this study, gas permeability measurements have not been corrected from Klinkenberg effect [7]. All the presented effective and "intrinsic" permeability in this article are apparent permeability. Since all the permeability measurements have been performed using the same static gas pressure P_i, the comparison of apparent and "intrinsic" permeability can then be considered as relevant. To make the notations more readable, the term apparent will be considered implicit in the following.

In order to measure the effective gas permeability at a given water saturation, the sample is first saturated and conditioned according to the protocol described in the previous section. The quasi-steady flow state method is then used to measure the effective permeability to gas.

The relative gas permeability for a given liquid saturation state, denoted $K_{r,g}(S_w)$, is estimated by dividing the effective gas permeability at the saturation of the sample $K_{eff,g}$ by the intrinsic gas permeability measured in dry state $K_{i,g}$:

$$K_{r,g}(S_w) = \frac{K_{eff,g}(S_w)}{K_{i,g}} \qquad \text{(eq. 5)}$$

The experimental protocol aims at keeping measurement uncertainties as low as possible. The flow rate measurement using the pressure variation in a constant volume is accurate, and usually used to calibrate commercial flow meter apparatus. Moreover, the possibility of using various tank volumes V_t (Figure 1) allows to maintain the flow rate measurement accuracy for a wide range of gas permeability. The main source of measurement error is attributed to the variation of temperature during measurement. Therefore, adequate temperature regulation equipment has been installed and allows obtaining reproducible measurements with an accuracy of about ±2%.

RELATIVE PERMEABILITIES OF A TIGHT SANDSTONE FIELD

Reservoir description and characterization

The samples investigated in this study came from four cored wells located in a gas field of the Sbaa Basin, SW Algeria. This field presents a large range of rock types, from conventional fair permeability-medium porosity to "tight reservoir" with low to very low permeability and porosity.

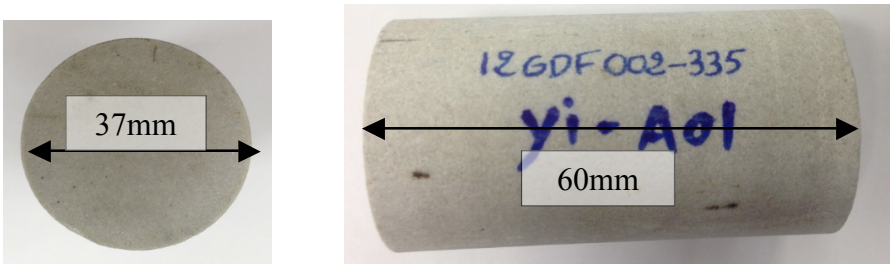

Figure 2: size and cross view of sample 2335

All samples were collected in the "tight reservoir" facies of the glaciogenic Ordovician formation. These are quartzitic sandstones with little detrital clay content varying from 0.3 to 12%, with rare heavy minerals and no feldspar. These rocks were deposited during the late Ordovician ice-house conditions period, in a glacial to subglacial environment [16]. They experienced a continuous burial during Paleozoic, reaching depth as deep as 4500m and temperature of more than 160°C during Carboniferous, leading to substantial porosity decrease by quartz overgrowth cementation or chemical compaction diagenetic processes. They were then uplifted during Hercynian orogeny, remaining in a relatively stable structural position during subsequent times up to present, and are now lying at depth ranging from 2000 to 2500m.

The samples are cylinders of 37 mm diameter and 60 mm long. Water porosity and "intrinsic" (dry) gas permeability ($K_{i,g}$) at 3 MPa of confining pressure have been measured (Table 1) for all samples. The water porosity varies between 1.5% and 5.0%, while the gas permeability ranges between 0.6-6 10^{-17} m^2, confirming that these samples can be considered as tight sandstones (see for examples [1, 6, 21]). Measurements of the pore size distribution (and cross check of porosity) were obtained through mercury intrusion porosimetry technique. The volume of the end trim samples is of the order of 2 to 3 cm^3. Given the low porosity of the tight sandstones, the volume of mercury injected into some samples is very small and the experiments must be interpreted with caution. Nevertheless, a fair agreement was globally obtained between the MIP porosity and the sample water porosity independent measurements considering that the end trim properties can vary from the sample it is extracted from (Table 1). The MIP porosity appears systematically higher than the sample porosity measured through water saturation under vacuum.

Table 1: porosity and intrinsic gas permeability of the samples

Sample reference	Depth (m)	ϕ_w, Water porosity, (%)	ϕ_{MIP}, (%)	$k_{t,g,}$, Intrinsic gas permeability x(10^{-17} m^2)
2335	2358,95	4,96	5,44	3,80
3248	2180,60	3,37	5,27	2,81
3249	2080,25	3,83	5,38	0,66
3250	2197,15	3,88	5,17	2,24
3372	2500,70	2,05	3,28	6,23
3375	2495,68	2,93	4,3	4,19
3377	2511,47	1,81	2,82	3,19
3379	2516,38	1,52	3,21	2,29
4456	2311,70	2,54	4,32	1,36
4458	2310,75	2,78	4,82	1,29

Gas relative permeability at low confinement

Concerning tight sands, numerous experimental studies have been carried out to estimate the gas relative permeability [5, 2, 18, 19], which is most of the time estimated without confinement or at low confining pressure. These results show a strong decrease in relative gas permeability for a low water saturation value, typically of the order of 0.3-0.4.

All the samples considered in this study show this trend at 3 MPa of confining pressure (Figure 3). For a water saturation S_w around 0.2, the gas relative permeability is reduced by more than 40% and for a saturation S_w around 0.4 the gas relative permeability reduction reaches a factor of 10 for most of the samples.

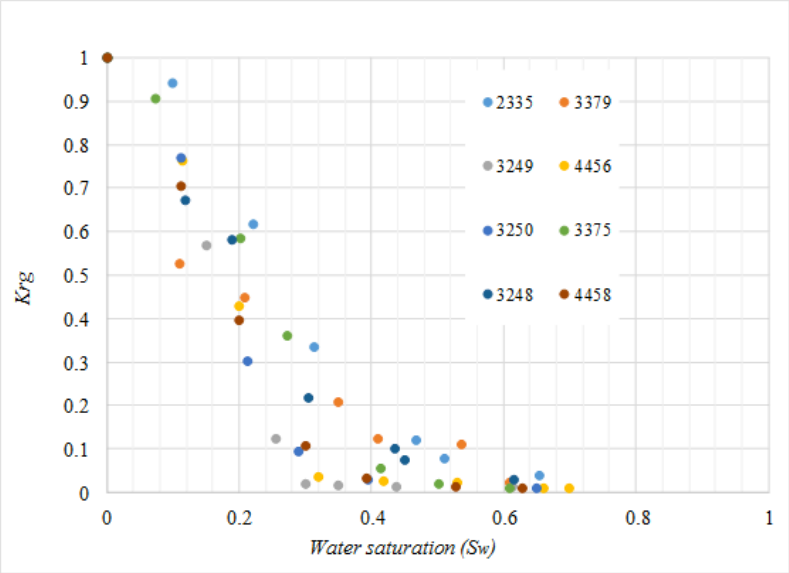

Figure 3 : Relative gas permeability under 3 MPa of confining pressure

This sensitivity to saturation is mainly attributed to the pore network structure composed of inter-grain pores connected by tight joints or cracks with an opening of the order of 0.01 µm to 1 µm [4]. The gas relative permeability of tight sandstone seems mainly dominated by the effect of these micro-cracks and joints, which control the flow in the porous network. As water saturation increases, the micro-cracks, which correspond to the smallest connected pathways, are the first to be water saturated. Then some pathways originally allowing the flow of the gas are likely to be blocked by the presence of water. The strong decrease of relative gas permeability, when compared to more permeable sandstones, reflects the fact that the gas percolating network disappears rapidly, as water saturation increases.

Increasing loading pressure is suspected to close easily tight joints and cracks and also induce a redistribution of the fluid phases in the pore network. Thus, the gas relative permeability may also depend on confinement. Nevertheless, this effect on tight gas relative permeability has not been widely studied probably because of the experimental

difficulties inherent to the measurements on tight samples. This is the goal of the next section; to evaluate gas relative permeability at different loading pressure.

Gas relative permeability as a function of confinement

The gas relative permeability is defined as the ratio of the effective gas permeability for a given saturation (S_w) and confinement (P_c), and the dry permeability under the same confinement:

$$K_{r,g}(S_w, Pc; Pc) = \frac{K_{eff,g}(S_w, Pc)}{K_{i,g}(Pc)} \quad \text{(eq. 6)}$$

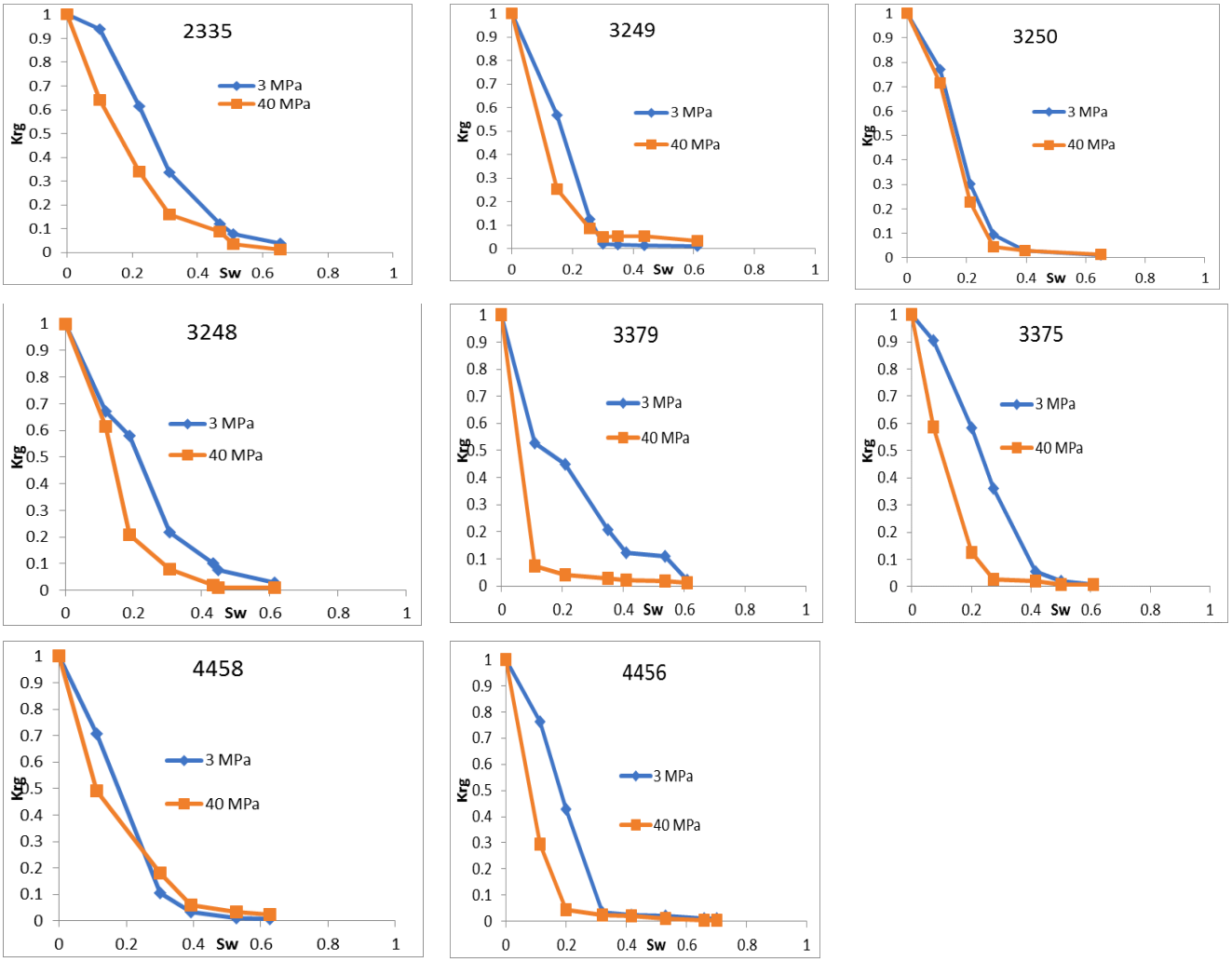

Figure 4: Relative gas permeability under confining pressures of 3MPa and 40MPa

Figure 4 highlights the dependence of the gas relative permeability on the mechanical loading for the eight samples studied. Relative gas permeability curves are shown for two different confining pressures of 3 MPa and 40 MPa. For all samples, apart sample 4458, gas relative permeability is reduced with increasing confining pressure and the gas residual saturation (through permeability "jail") is also shifted (the saturation end point of

gas relative permeability under loading at 40 MPa arises at a lower water saturation than for the case loaded at 3 MPa).

To better view the combined effect of both saturation and loading pressure, we define an effective gas relative permeability normalized by the intrinsic dry permeability at 3 MPa. denoted $K_{erg}(S_w, P_c; 3\ MPa)$

$$K_{erg}(S_w, P_c; 3\ MPa) = \frac{K_{eff,g}(S_w, P_c)}{K_{i,g}(3\ MPa)} \qquad \text{(eq. 7)}$$

For sandstones with low permeability, "jail" is identified in the literature [4] as the range of saturation where the gas and water relative permeability are less than 2%. The Figure 5 shows the effective relative gas permeability at different loading and the 2% criterion motivated by ”permeability jail” studies.

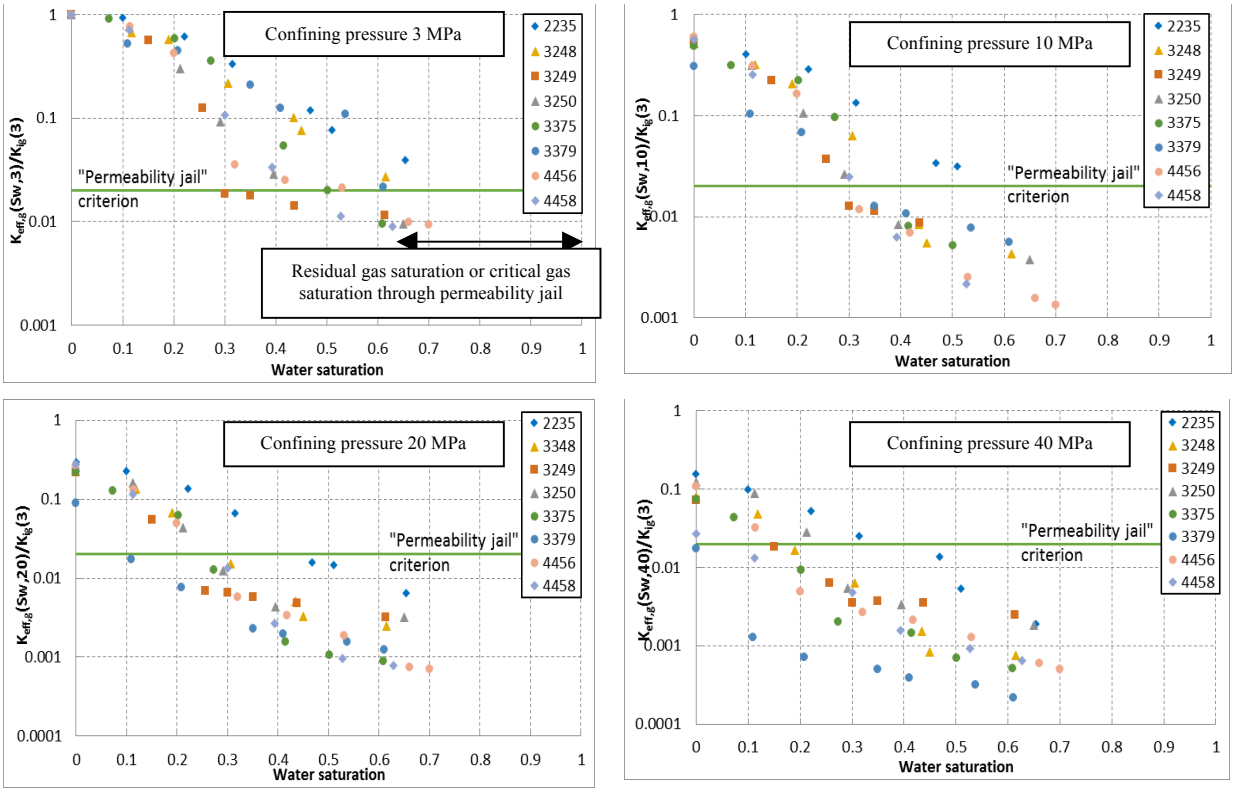

Figure 5: $K_{eff,g}(S_w,P_c)/K_{i,g}(3MPa)$ and “2% permeability jail” criterion (solid line).

These experimental results show that the relative permeability for tight rocks is sensitive to loading. The usual approximation in reservoir studies, which consists in considering only the influence of the loading on the absolute permeability and not on the relative permeabilities may then be a significant source of error.

Residual or critical gas saturation under low confinement (3 MPa)

Sticking to the objective of finding reliable and easily measurable parameters that allow predicting the behavior of sandstones rocks partially saturated and under mechanical

loading, we focus in this section on the lowest confining pressure (i.e. 3 MPa). We make the assumption that 3 MPa of confinement does not significantly modify the porous network when compared to the stress-free state.

For each sample, the "threshold saturation" is defined by the saturation of "permeability jail" occurrence (Table 2). These threshold saturations cover a large range of values depending on the sample (Table 2). This dispersion should be related to the differences in porous structure between samples.

Table 2: Threshold saturation for « permeability jail » (Threshold saturations are estimated from the shape of the curve).*

Reference	*2335*	*3248*	*3249*	*3250*	*3375*	*3379*	*4456*	*4458*
3 MPa	*0,72**	*0,68**	*0,30*	*0,48*	*0,50*	*0,61*	*0,53*	*0,45*

A first attempt to predict this threshold saturation is to correlate water porosity and the 2% threshold saturation under low confinement (Figure 6). However, it appears that there is no correlation between critical saturation and water porosity. The porosity accessible to water represents only the amount of porous volume connected and does not provide enough information on the connectivity of the porous network or on the size of the pore threshold. Those two last characteristics are much more susceptible to be linked to the "permeability jail" phenomenon.

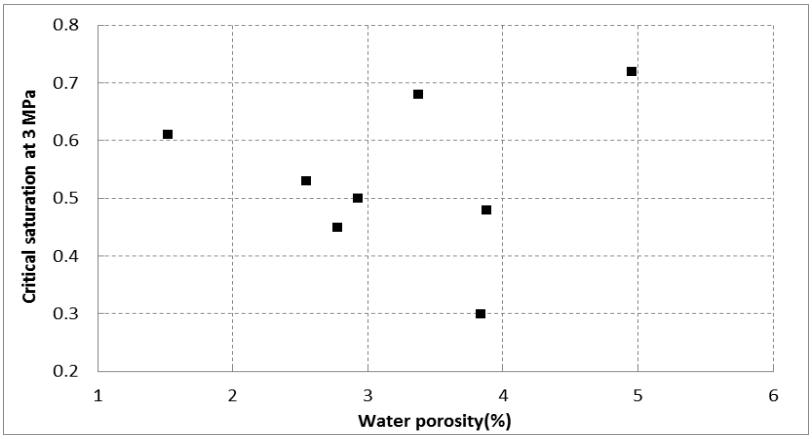

Figure 6: Critical saturation under 3 MPa of confining pressure as a function of water porosity.

The mercury intrusion porosimetry (MIP) provides a measurement of the porous structure and connectivity in unloaded conditions. As there is a fairly good correlation between the porosity measured by mercury porosimetry and that measured with water, we will therefore assume that there is also a correlation between mercury and water saturations for a given saturated pore size. The mercury injected into the porous network is a non-wetting fluid and begins by filling the larger pores. We can then use mercury porosimetry results to interpret and explain threshold saturations dispersion. On one hand, using the

critical saturations of "permeability jail" (Table 2) and the pore size distribution obtained by mercury porosimetry, it is possible to estimate the critical pore size (Table 3) associated to the threshold saturation, for which the pore network no longer percolates gas, i-e “permeability jail” has been reached.

Table 3: Pore size at the critical saturation of « permeability jail » under 3 MPa of confining pressure.

Sample reference	Threshold saturation	Pore diameter (µm)	Sample reference	Threshold saturation	Pore diameter (µm)
2335	0,72	0,68	3375	0,50	0,58
3248	0,68	0,80	3379	0,61	0,80
3249	0,30	0,23	4456	0,53	0,36
3250	0,48	0,55	4458	0,45	0,40

On the other hand, APEX represents the pore inlet diameter for which porous network connectivity is reached [14] and may be graphically determined using MIP results (Table 4). According to the APEX definition, when the size of the pore opening which controls the permeability is close to the pore size of the APEX, the porous network loses its connectivity. Indeed, a fairly good correlation between the pore size associated to the appearance of permeability “jail” (see Table 4) with APEX pore size (Figure 7) is obtained (permeability “jail” pore size around 80% of APEX pore size).

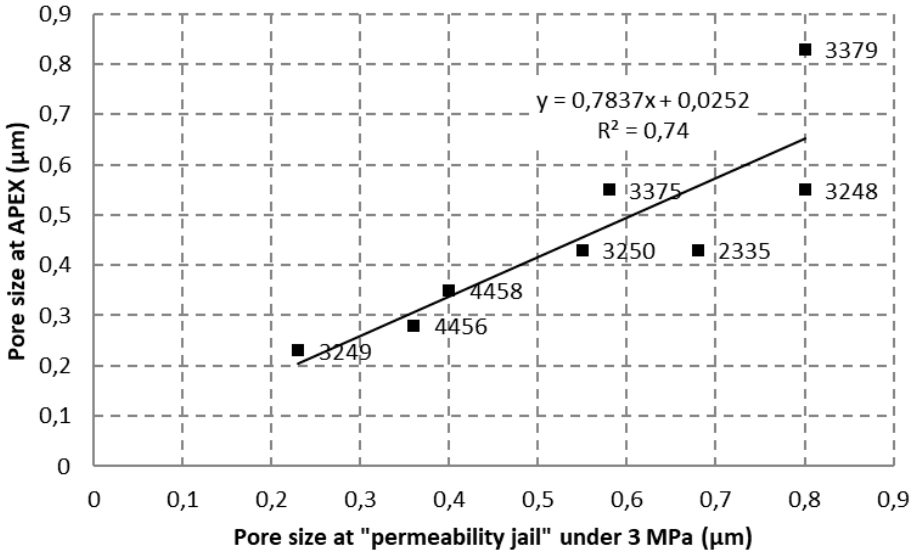

Figure 7: Correlation between pore size of « permeability jail » at 3 MPa and APEX pore size.

Thus, the MIP curves could be used before any relative permeability measurements to predict the water saturation likely to cause an hydraulic cut-off at low confinement as shown in Figure 7.

However, keeping in mind that the objective is to predict the apparition of “permeability jail” in in-situ conditions, the pore network characteristics for higher confining pressure

need to be known in order to predict saturation threshold at this confining pressure. A perspective to better characterize threshold saturations under loading would be to measure capillary pressure under loading or to estimate it using pore network modelling.

Table 4: Pore size at the APEX

Sample reference	APEX diameter (μm)	Sample reference	APEX diameter (μm)
2335	0,43	3375	0,55
3248	0,55	3377	0,55
3249	0,23	3379	0,83
3250	0,43	4456	0,28
3372	0,67	4458	0,35

CONCLUSIONS

Tight reservoirs, due to their high capillary pressures, have a very wide transition zone. Uncertainty about gas mobility may be responsible for incorrect evaluation of the recovery factor. A non-negligible uncertainty in the evaluation of the tight gas potential is related to the gas mobility dependence on both loading and water saturation.

This experimental study shows that tight gas relative permeability is very sensitive to confinement. It may then be recommended to estimate tight gas relative permeabilities under loading, even if it remains time-challenging in the case of a reservoir study.

These experimental results have been interpreted in terms of connectivity of the porous network, which is dominated by micro-cracks and joints. Under 3 MPa confinement, the threshold saturation for a relative gas permeability of 2% was successfully correlated with the APEX pore size determined from MIP results. This correlation remains to be confirmed under higher loading and it may be useful to have a characterization of the pore network properties under loading to predict the threshold saturation under in-situ conditions. This will be the subject of future works using either correction of MIP curves or pore network modelling allowing for loading evolution.

REFERENCES

[1] Albrecht D. , Reitenbach V., Investigations on fluid transport properties in the North-German Rotliegend tight gas sandstones and applications, Environ Earth Sci, 73 (10), 2015, pp. 5791–5799.

[2] Byrnes A.P., Issues with gas relative permeability in low-permeability sandstones, in understanding, exploring, and developing tight-gas sands. 2008: Vail Hedberg. p. 63-76.

[3] Chowdiah P., Effects of pore water distribution and stress on the laboratory measurement of tight sandstone properties, 1986, SPE15120.

[4] Cluff R.M. and Byrnes A.P., Relative permeability in tight gas sandstone reservoirs-The "permeability jail" model, in SPWLA 51st Annual Logging Symposium. 2010. Perth, Australia: Society of Petrophysicists and Well-Log Analysts.

[5] Fu X., Agostini F., Skoczylas F., Jeannin L., Experimental study of the stress dependence of the absolute and relative permeabilities of some tight gas sandstones, International Journal of Rock Mechanics and Mining Sciences, 2015. 77: p. 36-43.

[6] Gao H. and Li H.A., Pore structure characterization, permeability evaluation and enhanced gas recovery techniques of tight gas sandstones, J Nat Gas Sci Eng, 28 (2016), pp. 536–547.

[7] Klinkenberg L.J., The permeability of porous media to liquids and gases, in drilling and production practice. 1941. New York: American Petroleum Institute.

[8] Meziani H. and Skoczylas F., An experimental study of the mechanical behaviour of a mortar and of its permeability under deviatoric loading. Materials and Structures, 1999. 32(6): p. 403-409.

[9] Nooruddin H.A., Hossain M.E., Al-Yousef H., Okasha T., Comparison of permeability models using mercury injection capillary pressure data on carbonate rock samples, Journal of Petroleum Science and Engineering, 2014. 121: p. 9-22.

[10] Rilem T., 116-PCD: Permeability of Concrete as a Criterion of its Durability, Materials and Structures, 1999. 32(4): p. 174-179.

[11] Thomas R.D. and Ward D.C., Effect of overburden pressure and water saturation on gas permeability of tight sandstone cores. Journal of Petroleum Technology, 1972. 24(2): p. 120-124.

[12] Byrnes, A.P., Reservoir characteristics of low-permeability sandstones in the Rocky Mountains. The Mountain Geologist, 1997. 34(1): p. 39-51.

[13] Shanley K.W., Cluff R.M., and Robinson J.W., Factors controlling prolific gas production from low-permeability sandstone reservoirs: Implications for resource assessment, prospect development, and risk analysis, 2004, AAPG bulletin, 88(8):1083-1121.

[14] Swanson B.F., A simple correlation between permeabilities and mercury capillary pressures, Journal of Petroleum Technology, 1981. 33(12): p. 2498-2504.

[15] Skoczylas F., Ecoulements et couplages fluide-squelette dans les milieux poreux: études expérimentales et numériques, 1996, Université de science et technologie de Lille: Lille.

[16] Tournier F., Pagel M., Portier E., Wazir I., & Fiet N., Relationship between deep diagenetic quartz cementation and sedimentary facies in a late Ordovician glacial environment (Sbaa Basin, Algeria), Journal of Sedimentary Research, 2010, v.80, 1068-1084, DOI:10.2110/jsr.2010.094.

[17] Walsh J.B., Brace W.F., The effect of pressure in porosity and the transport properties of rock, Journal of Geophysical Research, 1984, v.89(B11), 9425-9431

[18] Wang Y., Chen Z., Morah V., Knabe R.J. and Appel M., Gas phase relative permeability characterization on tight gas samples, SCA2011-13.

[19] Ward J.S., Morrow N.R., Capillary pressure and gas relative permeabilities of low permeability sandstone, 1987, SPE 13882-PA, Society of Petroleum Engineers Formation Evaluation.

[20] Warpinski N.R., Teufel L.W., Determination of the effective-stress law for permeability and deformation in low-permeability rocks, SPE formation evaluation, 1992, 7(02):123, 131.

[21] Zhu P., Lin C., Wu P., Fan R, Zhang H., Pu W., Permeability prediction of tight sandstone reservoirs using improved BP neural network, Open Petrol Eng Journal, 8 (1) , 2015, pp. 288–292.